Supplementary Note 1: DNA-PAINT background

The greatest weakness of DNA-PAINT is that unbound imager probes contribute large amounts of background fluorescence which can drown out the signal peaks of individual bound probe molecules. The average background level b per area can be estimated as

$$b = \beta \cdot c \cdot \xi \qquad \textbf{(Suppl. Eq. 1)}$$

where β is the molecular brightness (i.e. the detected number of photons per second per probe molecule), c is the concentration of imager probes, and ξ is the thickness of the observed volume.

Regular DNA-PAINT relies on (1) low probe concentrations c, and (2) optical sectioning, such as total internal reflection fluorescence (TIRF) illumination, to minimize ξ [1]. Regular DNA-PAINT is usually incompatible with widefield illumination due to the large illumination and detection thickness ξ which leads to very high background b.

Even when minimizing ξ by optical sectioning, the probe concentration c usually is limited to 5 nM to keep the background fluorescence at an acceptable level [1, 2]. Low concentrations, however, have a detrimental effect on the imaging speed: the blinking rate or binding on-rate r_{on} can be estimated as

$$r_{on} = k_{on} \cdot c \qquad \textbf{(Suppl. Eq. 2)}$$

where k_{on} is the rate constant of an imager probe binding a docking strand.

Supplementary Note 2: DNA-PAINT imaging speed

The speed of SMLM depends on the time it takes to collect a sufficient number of blinks from every target with the additional caveat that a blink is only useful if it is spatially isolated from other blinks so that it can be correctly identified. Using a binomial distribution model, the probability of detecting x blinks within a diffraction area at any particular time can be predicted from the number of molecular targets (or docking strands; n) and the duty cycle (p):

$$P(X = x) = \binom{n}{x} \cdot p^x \cdot (1-p)^{n-x} \qquad \textbf{(Suppl. Eq. 3)}$$

Here, the duty cycle is defined as the ratio of the total accumulated blinking time for a single emitter and total observation time, or as the ratio of average on-time (t_{on}) of a molecule divided by the sum of average on-time and average off-time ($t_{on} + t_{off}$). For PAINT, it can alternatively be calculated as the binding on-rate ($r_{on} = 1/t_{off}$; proportional to probe concentration) divided by the sum of on- and off- ($r_{off} = 1/t_{on}$) rates:

$$\begin{aligned} p &= \frac{t_{on}}{t_{on} + t_{off}} \\ &= \frac{r_{on}}{r_{on} + r_{off}} \end{aligned} \qquad \textbf{(Suppl. Eq. 4)}$$

With these basic premises, we can investigate the effect of these parameters on imaging duration analytically to understand constraints in speed for regular DNA-PAINT and how to overcome them (**Suppl. Fig. 1**).

As a model for SMLM sampling, $P(X = 1)$ estimates the probability of only a single emitter blinking, whereas $P(X > 1)|P(X > 0)$ estimates the fraction of multi-emitter artifacts, i.e. the fraction of blinking events that consists of multiple emitters detected simultaneously within a diffraction-limited volume (**Suppl. Fig. 1c,e**). Assuming each

frame represents an observation, then the average imaging duration (number of frames) required to detect a number of blinks equal to the molecular targets is $n/P(X=1)$. Although we use this here as an estimate of imaging duration, the actual number of frames needed to reliably reconstruct an image is much more complex to define and beyond the scope of this discussion. The imaging duration is minimized when $P(X=1)$ is maximized; however, this comes at the cost of a high rate of multi-emitter artifacts. The maximum acceptable multi-emitter artifact rate, for example 10%, presents a threshold and therefore dictates the optimal duty cycle and sets the lower limit for imaging duration.

Since both binding on- and off-rates are tunable in DNA-PAINT, there is an optimal ratio between on- and off-rates to achieve the optimal duty cycle and imaging duration (in frames). However, since imaging duration in units of time rather than frames is ultimately of interest, the imaging duration (T) can be added to the model based on the additional assumption that the frame rate (f) is always matched to the binding off-rate:

$$
\begin{aligned}
T &= \frac{n}{P(X=1)} \cdot \frac{1}{f} \\
&= \frac{n}{n \frac{r_{on}}{r_{on}+r_{off}} \left(\frac{r_{off}}{r_{on}+r_{off}}\right)^{n-1}} \cdot \frac{1}{r_{off}} \\
&= \frac{\left(\frac{r_{on}+r_{off}}{r_{off}}\right)^{n-1}}{\frac{r_{off} r_{on}}{r_{on}+r_{off}}} \\
&= \left(\frac{r_{on}+r_{off}}{r_{off}}\right)^{n} \cdot \frac{1}{r_{on}} \\
&= \left(1+\frac{r_{on}}{r_{off}}\right)^{n} \cdot \frac{1}{r_{on}}
\end{aligned}
\qquad \textbf{(Suppl. Eq. 5)}
$$

The model predicts that binding on- and off-rates need to be optimized in concert (**Suppl. Fig. 1d,f**; assuming an on-rate constant of 2.3×10^6 M^{-1} s^{-1}). Increasing the binding on-rate (i.e. by increasing the probe concentration) by itself quickly leads to an

unacceptable increase in the rate of multi-emitter artifacts; whereas increasing the binding off-rate alone gains minimal benefits as most of the frames will be blank.

Importantly, in DNA-PAINT, the maximum acceptable values for both binding on- and off-rates are limited by the signal-to-background ratio (i.e. the ratio between the fluorescence detected from bound vs. unbound probes). To reiterate, the binding on-rate is proportional to probe concentration whereas the blinking off-rate should be proportional to camera frame rate. A fluorogenic probe, by reducing background fluorescence, therefore pushes the acceptable limits of both the binding on- and off-rates allowing the use of higher probe concentrations and higher frame rate.

Our model also recapitulates the effect of different densities of molecular targets n. At a fixed blinking off-rate (e.g. the same probe/docking combination), the ideal probe concentration to minimize imaging duration and avoid multi-emitter artifacts decreases with increasing target density (**Suppl. Fig. 1a**). At a fixed probe concentration, higher off-rates (and correspondingly higher frame rates) are necessary with increasing target density to avoid multi-emitter artifacts (**Suppl. Fig. 1b**). Our imaging experiments, i.e. probe/docking strand affinity and probe concentration, were optimized based on predictions by this model.

Supplementary Note 3: Fluorogenic imager / docking system

We have demonstrated that self-quenching imager probes and partially mismatched docking strands provide an easy and effective method to implement fluorogenic DNA-PAINT. Here we provide our underlying rationale and a brief overview of how the two sets of imager probes and dockings strands were designed.

Design considerations:

Our goal for this study was specifically to eliminate the need for optical sectioning and achieve fast DNA-PAINT imaging. We therefore prioritized specific properties in our imager probes and docking strands accordingly.

Imager probes:

1. Unbound probes need to be as dark as possible, i.e. quenching efficiency needs to be high. This is the main determinant of how well these probes will perform without optical sectioning, and also sets the limit for the maximum probe concentration that can be used.
2. Secondary structures in the probes should be avoided to minimize any impact on k_{on}. For our needs, an overall increase in blinking rate (r_{on}) is achieved as long as the increase in maximum probe concentration (c) is larger than any potential decrease in k_{on} (**Suppl. Eq 2**).
3. Bound probes need to unquench sufficiently as to not compromise localization precision. In practice, the fluorogenic ratio rather than absolute fluorescence is important since excitation laser power can be increased to compensate for imperfect unquenching.

Docking strands:

1. The docking strand sequence needs to be optimized so that probe unbinding occurs quickly (high r_{off}) to allow for maximum camera frame rate and imaging speed.
2. Bound probes need to unquench sufficiently despite binding against a non-fully complementary docking strand sequence.
3. Undesired secondary structures in the docking strand also need to be avoided to maximize k_{on}.

Simultaneous multiplexed imaging:

1. The emission spectra of the probes should be well-resolved so that the probes are imaged only in their own color channel and their concentration can be optimized independently.
2. Cross-specific binding between the different sets of imager probes and docking strand need to be minimized as any cross-talk will not only lead to image artifacts in the final reconstruction, but also artificially inflates the observed probe duty cycle which limits the maximum probe concentration and imaging speed.

Design process:

Imager probes:

We selected fluorophores Cy3B and ATTO 643 for our probes based on their reported brightness and spectral separation. The basic requirement for our application is that their fluorescence is well suppressed when placed in proximity to a quencher (**Suppl. Fig. 3b**). In the final imager probe format, Cy3B was highly fluorogenic when paired with BHQ2, BHQ3 or IBFQ (**Suppl. Fig. 3c,** unbound vs. bound to fully complementary sequence), with the Cy3B/BHQ2 combination used in images acquired in this study. For ATTO 643, good fluorogenicity was observed with IBFQ (**Suppl. Fig. 3c**).

The sequence of imager probe A was based on the extension of the regular DNA-PAINT probe. Candidate sequences for the second probe were found using the design tool in NUPACK [3] with the specified goal of minimizing binding to both imager probe A and docking strand A. Sequences with a higher predicted probability in the lack of secondary structures were prioritized as a predictor of higher k_{on}. The final imager probe B sequence was selected based on also finding a suitable docking strand B, and

with NUPACK predicting minimal cross-specific interactions between the two sets of imager probes and docking strands.

Docking strands:

We developed a protocol for screening docking sequences with fast unbinding kinetics against imager probes (binding off rate >10 s^{-1}). By changing some of the criteria it is also possible to screen for docking strands with slower off-rates in the future.

Given that the docking strands will be 15 bases in length, and we wanted to only consider the 4 native DNA bases, there are ~1 billion possible sequence permutations. Fortunately, there is a wealth of literature and tools available on the thermodynamics of oligonucleotide hybridization [3, 4] which allowed us to drastically cut down on the number of candidates. Using this reduced candidate list, it was then feasible to test and select the docking strand that performed well in DNA-PAINT experiments.

Computational screening was performed in two steps. 1) The goal of the first step was to efficiently reject unsuitable sequences to generate a shortlist of <100 candidates based on fast-to-calculate parameters. 2) With the smaller list, it was then possible to curate a list of 8 candidates based on DNA secondary structure predictions.

The first computational screening step was performed by filtering on parameters calculated with Biopython [4] (**Suppl. Table 3**; shared on Github [5]). While individual filters are not great determinants, applying many of these weak filters allows rejection of sequences that have a higher probability of failure. Melting temperature, the main predictor of binding off-rate, was calculated using the nearest neighbor thermodynamics model [6] based on aligned imager probe and docking sequences. Although the model is inaccurate for pair of sequences with a large number of mismatches, it did not affect our ability to find sequences with the desired kinetics. Alignment analyses were used as a proxy to detect likelihood of malformed secondary structures. Results from different combinations of sequences were filtered on to minimize the likelihood of homo-dimer formation or cross-specific binding (for the two sets of imager probes / docking strands used in simultaneous multiplexed DNA-PAINT). Filter thresholds were tuned to generate a shortlist of ~50-100 sequences.

The shortlist was further refined based on secondary structure analyses with NUPACK. The docking strands were evaluated based on the following criteria:

1) The most energetically favorable secondary structure between the imager and docking strand is approximately aligned (at 0°C and 0.5 M NaCl; **Suppl. Fig. 3d**).
2) The predicted free energy is comparable to a pair of 6-bp fully complementary sequences (**Suppl. Table 4; ~-11 kcal/mol**).
3) Negligible concentrations of undesired complexes were predicted.

The final candidates from this computational screening are listed in **Suppl. Table 4**. The final docking strands for each of the two probes were selected based on their performance in a qualitative manner when tested in DNA-PAINT experiments. For testing, docking strand sequences were conjugated to secondary antibodies, typically with one or two bases added at the terminals as padding (lack of secondary structures were reverified with NUPACK).

Supplementary Tables

	5’ to 3’ direction
Biotin handle	DNA origami - CGGTTGTACTGTGACCGATTC
Biotin conjugated anti-handle	GAATCGGTCACAGTACAAC - Biotin

Supplementary Table 1

ssDNA handles for DNA origami attachment to coverslips.

	5’ to 3’ direction
Cy3B strand	Cy3B - AGAAGTAATGTGGAA
Cy3B quencher adapter	TTCCACATTACTTCTGTTATTGGTGTAGCG
ATTO 643 strand	ATTO 643 - AAGAAGTAAAGGGAG
ATTO 643 quencher adapter	CTCCCTTTACTTCTTGTTATTGGTGTAGCG
Quencher strand	CGCTACACCAATAAC – Que Where Que is BHQ1, BHQ2, BHQ3, Dabcyl, Iowa Black FQ (IBFQ), or Iowa Black RQ (IBRQ).

Supplementary Table 2

Oligonucleotides used for fluorophore-quencher testing assays.

	Docking strand criteria	Threshold
1	5’ matching length	≥ 3 bases
2	3’ matching length	≥ 3 bases
3	Melting temperature (Tm)	-35 to -25 °C
4	Number of alignments	≤ 2
5	Highest alignment score	≥ 9
6	Lowest number of sub-sequences in alignments	1
7	Self-dimer melting temperature	< Tm -15 °C
8	Highest self-dimer alignment score	≤ 7
9	Off-target melting temperature	< Tm -15 °C
10	Highest off-target alignment score	≤ 7

Supplementary Table 3

List of criteria for screening suitable docking strands.

Imager probe	Docking Candidate		Free Energy (kcal/mol)	DNA-PAINT
Imager probe A	I	TTCAACATATCCTCT	-10.26	Poor kinetics / fluorescence
	II	TTCTTCAATATTTCT	-10.46	Final docking strand
	III	TTCATCAATATTTCT	-10.89	Untested
	IV	TTCAACATCTCCTCT	-10.17	Untested
	V	TTCTATAATCCTTCT	-10.60	Untested
	VI	TTCATCAATACATCT	-10.97	Untested
	VII	TTCTAAATCCCTTCT	-11.20	Untested
	VIII	TTCTTTCTTACATCT	-9.98	Untested
Imager probe B	I	CTCTCTGAACGGCTT	-10.60	Poor kinetics / fluorescence
	II	CTGCCTGGACGCCTT	-11.97	Poor kinetics / fluorescence
	III	CTCGCTGCCCCTCTT	-10.97	Poor kinetics / fluorescence
	IV	CTGCCTTCGCGCCTT	-11.54	Poor kinetics / fluorescence
	V	CTCGCTGAACCCCTT	-12.55	Final docking strand
	VI	CTCGCTAGACCCCTT	-12.55	Untested
	VII	CTGCCTAGACGTGTT	-10.47	Untested
	VIII	CTCGCTGGACCCCTT	-12.55	Untested

Supplementary Table 4

List of docking strand candidates.

Supplementary Figures

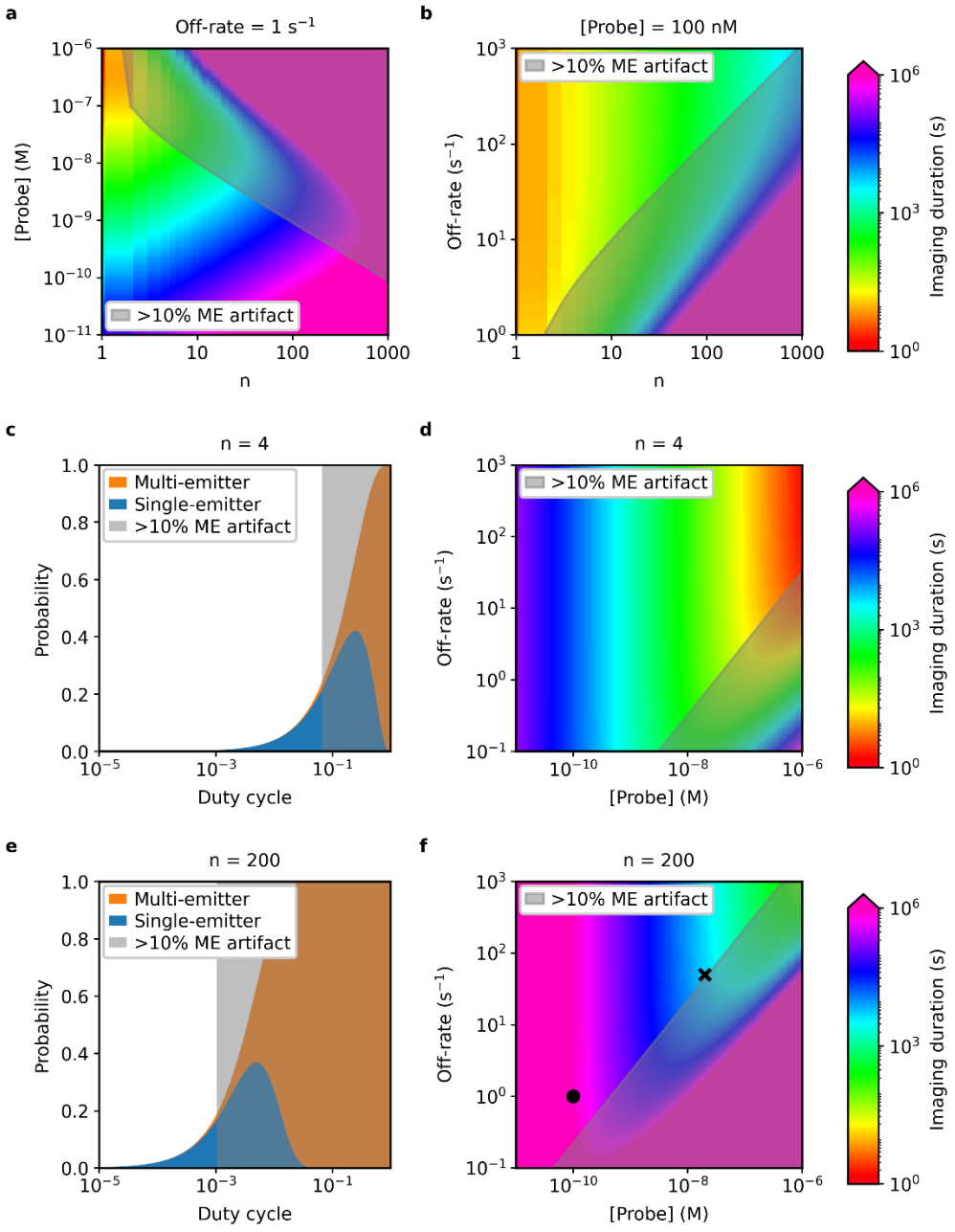

Supplementary Figure 1

Prediction of DNA-PAINT imaging speed based on a binomial distribution model of blinking. **(a)** For a constant binding off-rate, the optimal imager probe concentration decreases as the number of docking strands in a diffraction-limited area (n) increases. **(b)** For a given constant probe concentration (and binding on-rate), the optimal off-rate increases as the number of docking strands in a diffraction-limited area increases. **(c)** A relatively high duty cycle is optimal (6.6%) if there are only n=4 docking strands per diffraction-limited area. The upper limit is bound by the need to avoid multi-emitter artifacts. **(d)** Probe concentration and binding off-rate need to be optimized together to minimize imaging duration. For both regular DNA-PAINT (expected off-rate ~1 s^{-1}) and our fluorogenic probe (off-rate ~50 s^{-1}), the optimal probe concentration of ~30 and ~1,500 nM, respectively, is above what we and others have found to be acceptable from a signal-to-background perspective (>5 and >250 nM, respectively). **(e)** A low duty cycle is optimal (0.1%) if there is a high number of docking strands (e.g. n=200) per diffraction-limited area (e.g. antibody labeled microtubule). **(f)** At this docking strand density, in contrast to the n=4 scenario, the optimal probe concentration of ~0.5 and ~20 nM, respectively, lies well below the limits dictated by background. Imaging speed is instead limited by the 'slow' binding off-rate with this type of samples when performing fast fluorogenic DNA-PAINT. Conditions used for the experiments presented in **Fig. 3** are indicated (circle: regular DNA-PAINT; cross: fast fluorogenic DNA-PAINT). The imaging speed was increased by increasing both probe concentration and binding off-rate while maintaining multi-emitter artifacts at an acceptable level.

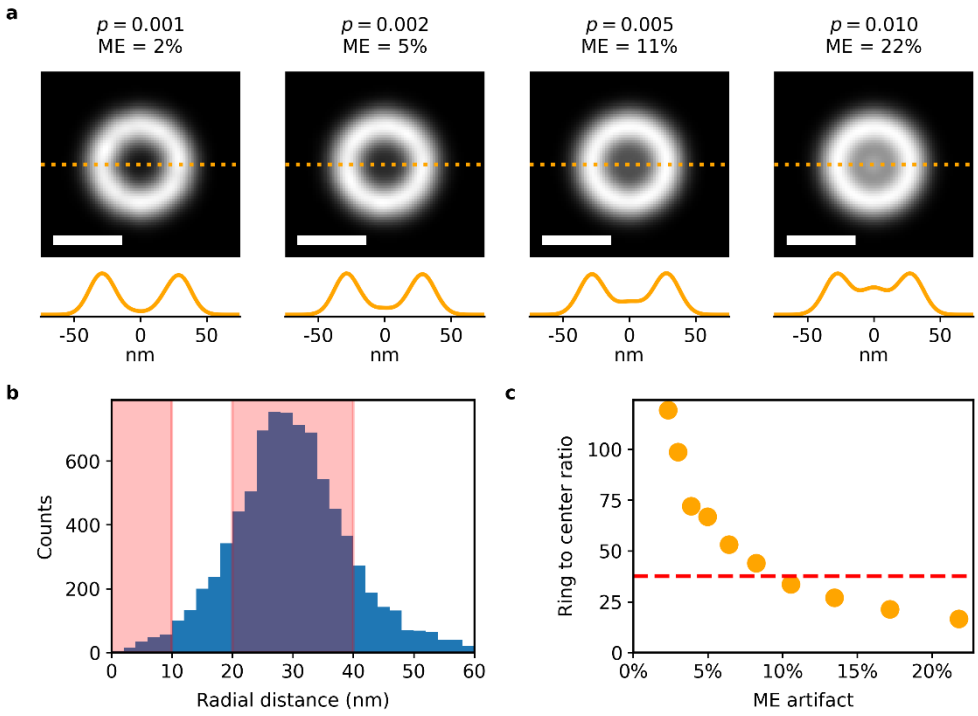

Supplementary Figure 2

(a) Simulation of blinking events on a ring structure (radius = 30.2 nm; docking strands = 48; localization precision = 8.1 nm; observations = 1,000,000) based on a binomial distribution model as described in **Suppl. Note 2**. As duty cycle (p) increases, the chance of multi-emitter (ME) artifacts increases which is observed as the erroneous filling in of the ring center. Scale bar is 50 nm. **(b)** This effect was quantified by the ratio of blinking events on the ring (radial distance 20-40 nm; red) versus those in the center (radial distance <10 nm; red). The graph was generated from the origami ring experimental data presented in **Fig. 2**. **(c)** Calibration points were generated from the simulated data (orange). A ring to center ratio of 37 was calculated from the experimental data (red dash) which estimates the occurrence of multi-emitters at ~9%.

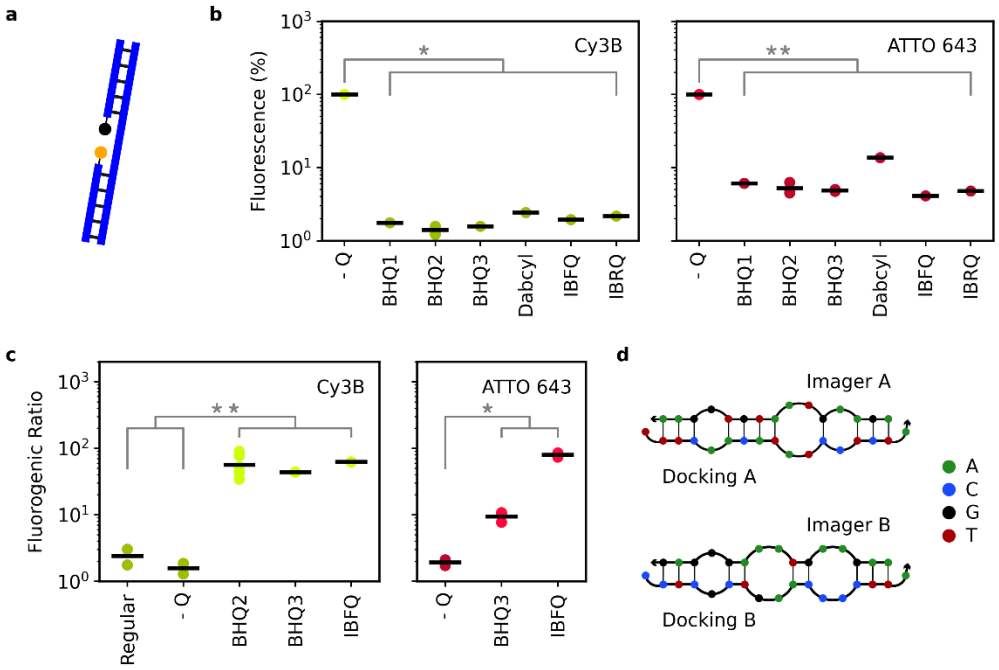

Supplementary Figure 3

(a) Diagrammatic representation of the DNA complex formed to bring the fluorophore (yellow circle) and quencher (black circle) in close proximity for the experimental data presented in (b). **(b)** Data shows both Cy3B and ATTO 643 are well-quenched by various quenchers (BHQ1, BHQ2, BHQ3, Dabcyl, IBFQ, IBRQ; pooled, two-sided one-sample Wilcoxon signed-rank test against 100%, T-statistic=0, p=0.018 for Cy3B (*, n_{sample}=7; 1.8% ± 0.4%) and T-statistic=0, p=0.008 for ATTO 643 (**, n_{sample}=9; 6.0% ± 3.0%) respectively). **(c)** Regular DNA-PAINT probe or imager probe A without a quencher (- Q) are relatively non-fluorogenic in contrast to those conjugated with BHQ2, BHQ3 or IBFQ. Two-sided Mann-Whitney U test, U-statistic=0, p=0.004 (**), pooled no quencher (n_{sample}=4; 2.0 ± 0.7) versus with quencher (n_{sample}=8; 55.8 ± 19.5). Similarly, imager probe B is only weakly fluorogenic without a quencher. Two-sided Mann-Whitney U test, U-statistic=0, p=0.041 (*), pooled no quencher (n_{sample}=2; 1.9 ± 0.3) versus with quencher (n_{sample}=6; 37.5 ± 38.63). **(d)** Secondary structure predicted by NUPACK for imager probe and docking strand sets A and B (P1-0 and D1-1c, P2-0 and D2-1a; at 0°C and 0.5 M NaCl). Average statistics presented as mean ± SD.

References

1. Schnitzbauer, J., Strauss, M.T., Schlichthaerle, T., Schueder, F. & Jungmann, R. Super-resolution microscopy with DNA-PAINT. *Nature protocols* **12**, 1198-1228 (2017).

2. Lee, J., Park, S., Kang, W. & Hohng, S. Accelerated super-resolution imaging with FRET-PAINT. *Mol Brain* **10**, 63 (2017).

3. Zadeh, J.N. et al. NUPACK: Analysis and design of nucleic acid systems. *J Comput Chem* **32**, 170-173 (2011).

4. Cock, P.J. et al. Biopython: freely available Python tools for computational molecular biology and bioinformatics. *Bioinformatics* **25**, 1422-1423 (2009).

5. https://github.com/bewersdorflab/fluorogenic-dna-paint-manuscript-supplement/blob/main/imagerb_docking_strand_screen.ipynb (2022).

6. SantaLucia, J., Jr. A unified view of polymer, dumbbell, and oligonucleotide DNA nearest-neighbor thermodynamics. *Proceedings of the National Academy of Sciences of the United States of America* **95**, 1460-1465 (1998).